

Axiomatic/Asymptotic Analysis of Refined Layer-Wise Theories for Composite and Sandwich Plates

*Original*

Axiomatic/Asymptotic Analysis of Refined Layer-Wise Theories for Composite and Sandwich Plates / Petrolo, Marco; Lamberti, Alessandro. - In: MECHANICS OF ADVANCED MATERIALS AND STRUCTURES. - ISSN 1537-6532. - STAMPA. - 23:1(2016), pp. 28-42. [10.1080/15376494.2014.924607]

*Availability:*

This version is available at: 11583/2601761 since: 2020-04-24T13:51:32Z

*Publisher:*

Taylor & Francis Group

*Published*

DOI:10.1080/15376494.2014.924607

*Terms of use:*

This article is made available under terms and conditions as specified in the corresponding bibliographic description in the repository

*Publisher copyright*

Taylor and Francis postprint/Author's Accepted Manuscript

This is an Accepted Manuscript of an article published by Taylor & Francis in MECHANICS OF ADVANCED MATERIALS AND STRUCTURES on 2016, available at <http://www.tandfonline.com/10.1080/15376494.2014.924607>

(Article begins on next page)

# Axiomatic/asymptotic analysis of refined layer-wise theories for composite and sandwich plates

Marco Petrolo <sup>\*</sup>, Alessandro Lamberti <sup>†</sup>

Department of Mechanical and Aerospace Engineering, Politecnico di Torino, 10129 Torino, Italy

Accepted Paper:

Reference Number MAMS 09052013

*Author for correspondence:*

Marco Petrolo, Researcher Assistant,  
Department of Mechanical and Aerospace Engineering,  
Politecnico di Torino,  
Corso Duca degli Abruzzi 24,  
10129, Torino, Italy,  
tel: +39 011 090 6869,  
fax: +39 011 090 6899,  
e-mail: marco.petrolo@polito.it,  
website: www.mul2.com

---

<sup>\*</sup>Researcher Assistant, e-mail: marco.petrolo@polito.it

<sup>†</sup>PhD student, e-mail: alessandro.lamberti@polito.it

## ***Abstract***

*This paper deals with layer-wise (LW) models for composite and sandwich plates. Refined layer-wise models are built according to the Carrera Unified Formulation (CUF) which has been developed over the last decade for beams, plate and shell theories. CUF allows the hierarchical implementation of refined models based on any-order expressions of the unknown variables. In this paper, displacement variables are expanded along the layer thickness through Legendre polynomials. Comparisons with previous analysis based on Equivalent Single Layer (ESL) approaches are given. The effect of each term of the expansion on the accuracy of stress/displacement components for the static response of composite and sandwich plates is analyzed. Ineffective terms are discarded from the expansion in order to save computational cost. The reduced models obtained, which are denoted as mixed axiomatic/asymptotic models, are as accurate as full expansion models. Numerical analysis is restricted to closed-form solutions via Navier-type solutions. A number of problems related to laminated and sandwich structures are solved and related reduced models are built by varying geometrical, lay-up and mechanical parameters. Results show that in some cases (in particular those related to sandwich plates) reduced layer-wise models can save up to 50% of the degrees-of-freedom of the full models without significant accuracy losses. It is found that the significant terms related to reduced models are very much subordinated to the problems considered and that from that point of view the use of a framework that can generate any theory, such as CUF, appears very suitable to build reduced models for plates.*

Keywords: plate, layer-wise, composites, unified formulation, refined models

# 1 Introduction

During the last decades the analysis of structures has experienced a continuous development due to the need to analyze innovative structures, such as laminated and sandwich plates, and the possibilities offered by computer analysis. Refined plate/shell/beam models have been proposed to enhance the analysis capabilities of classical models such as Euler-Bernoulli and Timoshenko ([1, 2, 3] for beams and Kirchhoff and Reissner-Mindlin [4, 5, 6]) for plates.

This paper deals with advanced plate models for composite structures and, in the following, a brief overview of some of the most important contributions in this field is given. An in-depth analysis of plate models can be found in the excellent works written by Ambartsumian [7], Librescu and Reddy [8], Grigolyuk and Kulikov [9] and [10].

Structural models can be developed through axiomatic and asymptotic methods. The former are based on the intuition of scientists to create simplified kinematic models which neglect some characteristics of the mechanical behavior of a structure. For example, the Kirchhoff plate does not consider the shear effects and the thickness stretching. A further way to develop structural models is based on the asymptotic method through the expansion of characteristic parameters of the structures (e.g. the length-to-thickness ratio). Excellent works on the asymptotic method for plates and shells can be found in [11], [12], [13], [14], [15], [16], [17].

Plate models can be developed according to two main approaches, the Equivalent Single Layer (ESL) approach and the Layer Wise (LW) approach. The former models a laminated plate as a single "equivalent" lamina. The latter exploits independent variables in each layer, that is, independent kinematic assumptions can be considered in each layer. As the number of plies of a laminated plate increases the number of unknowns in ESL is constant and in LW increases. A comprehensive review of these models can be found in [18] where the author points out the main differences between ESL and LW models. According to the author, two main types of the LW approach exist, partial LW theories where only two in-plane displacement components are expanded, and the full LW approach, where all the displacement components are expanded. In addition the author highlights that a thick plate can be profitably analyzed by means of an LW approach rather than an ESL approach. The study of static, free vibration and buckling responses of general laminated thick composite plates was conducted by [19] where a layer-wise finite element method (FEM) was employed. An interesting application of LW approach for free vibration analysis of composite and sandwich plates can be found in [20]. In [21] the author considers a combination of a layer-wise approach and a multiquadrics discretization method in order to accurately predict the displacement field of laminated composite and sandwich plates. The LW approach can be profitably employed in order to account for multiple delaminations between layers as reported in [22]. Another interesting use of the LW approach can be found in [23] where the analysis of multi-layered plates with embedded/surface bonded piezoelectric/magnetostrictive layers was carried out employing the layer-wise mixed finite element method.

The present work is based on the Carrera Unified Formulation. CUF has been developed over the last decade for beams, plates and shells. In the CUF framework, the unknown variables are described via expansions of the thickness coordinate of the plate. The expansion order and type are free parameters of the analysis. Stiffness, mass and loading arrays are obtained through a set of fundamental nuclei whose form does not depend on either the expansion order nor on the choice made for the base functions. More details about CUF can be found in [24] and in the books by Carrera et alii [25, 26].

CUF has been successfully extended to LW [27, 28, 29]. In [30], analytical closed form solutions for the free vibration analysis of multilayered plates have been presented. In [31], the authors employ the LW approach and CUF model to analyze the linearized buckling of laminated plates. Whereas in [32] attention was paid to the analysis of sandwich plates by means of the LW and ESL approaches and CUF. The present work exploits the so-called mixed axiomatic/asymptotic method recently proposed by Carrera and Petrolo [33, 34]. This method is based on a preliminary axiomatic choice of a refined model obtained through CUF and, then, it allows us to evaluate the effectiveness of each higher-order term of a structural theory against a reference solution. Those variables whose influence cannot be neglected are retained. This leads to the development of reduced models whose accuracies are equivalent to those of full higher-order models. The influence of each term can be evaluated for different values of geometrical and material parameters, such as the thickness-to-length ratio or the orthotropic ratio in order to obtain asymptotic-like results. The mixed axiomatic has been recently applied to ESL plate [33, 35, 36] and beam [34, 37] models. In [36], this method was adopted to build the so-called Best Theory Diagram

where, for a given structural problem and a given accuracy, the structural model with the minimum number of unknown variables can be read.

The mixed axiomatic/asymptotic method is applied to LW plate models in this paper. This work is restricted to plate geometries, and is based on closed-form solutions and exploits the Principle of Virtual Displacement (PVD). This paper is organized as follows: a description of the adopted formulation is provided in Sec. 2; the strategy employed to evaluate the effectiveness of terms of various plate theories is presented in Sec. 3. Results and recommendations are reported in Sec 4. Conclusions are discussed in Sec. 5.

## 2 Carrera Unified Formulation

A brief overview of CUF is given in the following; more details can be found in [24], [25] and [26].

### 2.1 Equivalent Single Layer and Layer Wise approaches

According to CUF the displacement field of a structural model can be described as:

$$\mathbf{u} = F_\tau \mathbf{u}_\tau \quad \tau = 1, 2, \dots, N_{\text{EXP}} \quad (1)$$

where  $\mathbf{u}$  is the displacement vector,  $N_{\text{EXP}}$  is the number of terms of the expansion and  $\mathbf{u}_\tau$  are the unknown variables.  $F_\tau$  are Mc-Laurin functions of  $z$  defined as  $F_\tau = z^{\tau-1}$ , where  $z$  is the thickness coordinate (see Fig. 1). This approach can be seen as an Equivalent Single Layer method. In the following the ESL models are synthetically indicated as EDN, where N is the expansion order. An example of an ED4 displacement field is reported,

$$\begin{aligned} u_x &= u_{x1} + z u_{x2} + z^2 u_{x3} + z^3 u_{x4} + z^4 u_{x5} \\ u_y &= u_{y1} + z u_{y2} + z^2 u_{y3} + z^3 u_{y4} + z^4 u_{y5} \\ u_z &= u_{z1} + z u_{z2} + z^2 u_{z3} + z^3 u_{z4} + z^4 u_{z5} \end{aligned} \quad (2)$$

As mentioned in [33], classical models such as CLT and FSDT can be considered as special cases of full linear expansion (ED1). Another possible approach is the Layer Wise method which describes the displacement field of each single layer of a plate as

$$\mathbf{u}^k = F_t \cdot \mathbf{u}_t^k + F_b \cdot \mathbf{u}_b^k + F_r \cdot \mathbf{u}_r^k = F_\tau \mathbf{u}_\tau^k \quad \tau = t, b, r \quad r = 2, 3, \dots, N \quad k = 1, 2, \dots, N_l \quad (3)$$

where  $k$  is the generic  $k$ -layer of a plate and  $N_l$  is the number of the layers. Subscripts  $t$  and  $b$  correspond to the top and the bottom of a layer. Functions  $F_\tau$  depend on a coordinate  $\zeta_k$  whose range is  $-1 \leq \zeta_k \leq 1$ . Functions  $F_\tau$  are derived from the Legendre polynomials according to the following equations

$$F_t = \frac{P_0 + P_1}{2} \quad F_b = \frac{P_0 - P_1}{2} \quad F_r = P_r - P_{r-2} \quad r = 2, 3, \dots, N \quad (4)$$

The Legendre polynomials used for the fourth order theory are

$$P_0 = 1 \quad P_1 = \zeta_k \quad P_2 = \frac{3\zeta_k^2 - 1}{2} \quad P_3 = \frac{5\zeta_k^3 - 3\zeta_k}{2} \quad P_4 = \frac{35\zeta_k^4 - 15\zeta_k^2}{8} + \frac{3}{8} \quad (5)$$

LW models require the compatibility of displacement at the interfaces, that is

$$\mathbf{u}_t^k = \mathbf{u}_b^{k+1} \quad k = 1, \dots, N_l - 1 \quad (6)$$

In the following LW models are synthetically indicated as LDN, where N is the expansion order. An example of LD4 layer displacement field is

$$\begin{aligned} u_x^k &= F_t u_{xt}^k + F_2 u_{x2}^k + F_3 u_{x3}^k + F_4 u_{x4}^k + F_b u_{xb}^k \\ u_y^k &= F_t u_{yt}^k + F_2 u_{y2}^k + F_3 u_{y3}^k + F_4 u_{y4}^k + F_b u_{yb}^k \\ u_z^k &= F_t u_{zt}^k + F_2 u_{z2}^k + F_3 u_{z3}^k + F_4 u_{z4}^k + F_b u_{zb}^k \end{aligned} \quad (7)$$

More details on this approach can be found in [25].

## 2.2 Geometric and Constitutive Relations

The coordinate frame adopted is presented in Fig. 1. The lengths of the plate sides along  $x$  and  $y$  axes are indicated respectively as  $a$  and  $b$ . The thickness of the plate is denoted as  $h$ . The stresses,  $\sigma^k$ , and the strains,  $\epsilon^k$ , of the generic  $k$ -th layer are grouped as follows:

$$\begin{aligned} \sigma_p^k &= \{\sigma_{xx}^k \ \sigma_{yy}^k \ \sigma_{xy}^k\}^T, & \epsilon_p^k &= \{\epsilon_{xx}^k \ \epsilon_{yy}^k \ \epsilon_{xy}^k\}^T \\ \sigma_n^k &= \{\sigma_{xz}^k \ \sigma_{yz}^k \ \sigma_{zz}^k\}^T, & \epsilon_n^k &= \{\epsilon_{xz}^k \ \epsilon_{yz}^k \ \epsilon_{zz}^k\}^T \end{aligned} \quad (8)$$

Subscript  $n$  is related to the in-plane components, whereas  $p$  refers to the out-of-plane components. In the case of linear theory, the strain-displacement relations are

$$\epsilon_p^k = \mathbf{D}_p^k \mathbf{u}^k \quad \epsilon_n^k = \mathbf{D}_n^k \mathbf{u}^k = (\mathbf{D}_{n\Omega} + \mathbf{D}_{nz}) \mathbf{u}^k \quad (9)$$

with

$$\mathbf{D}_p = \begin{bmatrix} \frac{\partial}{\partial x} & 0 & 0 \\ 0 & \frac{\partial}{\partial y} & 0 \\ \frac{\partial}{\partial y} & \frac{\partial}{\partial x} & 0 \end{bmatrix} \quad (10)$$

$$\mathbf{D}_{n\Omega} = \begin{bmatrix} 0 & 0 & \frac{\partial}{\partial x} \\ 0 & 0 & \frac{\partial}{\partial y} \\ 0 & 0 & 0 \end{bmatrix} \quad (11)$$

$$\mathbf{D}_{nz} = \begin{bmatrix} \frac{\partial}{\partial z} & 0 & 0 \\ 0 & \frac{\partial}{\partial z} & 0 \\ 0 & 0 & \frac{\partial}{\partial z} \end{bmatrix} \quad (12)$$

In the case of orthotropic materials, the following constitutive law holds:

$$\sigma^k = \mathbf{C}^k \epsilon^k \quad (13)$$

According to Eqs. 8, the previous equation becomes

$$\sigma_p^k = \tilde{\mathbf{C}}_{pp}^k \epsilon_p^k + \tilde{\mathbf{C}}_{pn}^k \epsilon_n^k \quad \sigma_n^k = \tilde{\mathbf{C}}_{np}^k \epsilon_p^k + \tilde{\mathbf{C}}_{nn}^k \epsilon_n^k \quad (14)$$

where matrices  $\tilde{\mathbf{C}}_{pp}^k$ ,  $\tilde{\mathbf{C}}_{nn}^k$ ,  $\tilde{\mathbf{C}}_{pn}^k$  and  $\tilde{\mathbf{C}}_{np}^k$  are

$$\tilde{\mathbf{C}}_{pp}^k = \begin{bmatrix} \tilde{C}_{11} & \tilde{C}_{12} & \tilde{C}_{16} \\ \tilde{C}_{12} & \tilde{C}_{22} & \tilde{C}_{26} \\ \tilde{C}_{16} & \tilde{C}_{26} & \tilde{C}_{66} \end{bmatrix}^k \quad (15)$$

$$\tilde{\mathbf{C}}_{nn}^k = \begin{bmatrix} \tilde{C}_{55} & \tilde{C}_{45} & 0 \\ \tilde{C}_{45} & \tilde{C}_{44} & 0 \\ 0 & 0 & \tilde{C}_{33} \end{bmatrix}^k \quad (16)$$

$$\tilde{\mathbf{C}}_{pn}^k = \tilde{\mathbf{C}}_{np}^k = \begin{bmatrix} 0 & 0 & \tilde{C}_{13} \\ 0 & 0 & \tilde{C}_{23} \\ 0 & 0 & \tilde{C}_{36} \end{bmatrix}^k \quad (17)$$

For the sake of brevity, the dependence of the elastic coefficients  $[\tilde{C}]_{ij}^k$  on Young's modulus, Poisson's ratio, the shear modulus and the fiber angle is not reported. It can be found in [38] or [18].

## 2.3 Governing Differential Equations

The governing equations are obtained via the Principle of Virtual Displacement (PVD),

$$\sum_{k=1}^{N_l} \int_{\Omega_k} \int_{A_k} \left( \delta \epsilon_p^{kT} \sigma_p^k + \delta \epsilon_n^{kT} \sigma_n^k \right) d\Omega_k dz = \sum_{k=1}^{N_l} \delta L_e^k \quad (18)$$

The integration domains  $\Omega_k$  and  $A_k$  indicate the reference plane of the lamina and its thickness. The term  $\sum_{k=1}^{\bar{N}_l} \delta L_e^k$  indicates the virtual variation of the work of the external loadings. CUF approach applied to Eq. 18 leads to governing equations given in terms of fundamental nuclei which are formally independent of the expansion order  $N$  and the description of the variables (LW or ESL). Using Eqs. 9 and 14, Eq. 18 becomes

$$\int_{\Omega_k} \int_{A_k} \left\{ (\mathbf{D}_p \delta \mathbf{u}^k)^T [(\mathbf{C}_{pp}^k \mathbf{D}_p + \mathbf{C}_{pn}^k (\mathbf{D}_{np} + \mathbf{D}_{nz})) \mathbf{u}^k] + ((\mathbf{D}_{np} + \mathbf{D}_{nz}) \delta \mathbf{u}^k)^T [(\mathbf{C}_{pn}^{kT} \mathbf{D}_p + \mathbf{C}_{nn}^k (\mathbf{D}_{np} + \mathbf{D}_{nz})) \mathbf{u}^k] \right\} d\Omega_k dz = \delta L_e^k \quad (19)$$

Using equation 3 the previous equation can be written as:

$$\int_{\Omega_k} \int_{A_k} \left\{ (\mathbf{D}_p (F_s \delta \mathbf{u}_s^k))^T [(\mathbf{C}_{pp}^k \mathbf{D}_p + \mathbf{C}_{pn}^k (\mathbf{D}_{np} + \mathbf{D}_{nz})) (F_\tau \mathbf{u}_\tau^k)] + ((\mathbf{D}_{np} + \mathbf{D}_{nz}) (F_s \delta \mathbf{u}_s^k))^T [(\mathbf{C}_{pn}^{kT} \mathbf{D}_p + \mathbf{C}_{nn}^k (\mathbf{D}_{np} + \mathbf{D}_{nz})) (F_\tau \mathbf{u}_\tau^k)] \right\} d\Omega_k dz = \delta L_e^k \quad (20)$$

The following notation is introduced

$$(E_{\tau s}, E_{\tau, z s}, E_{\tau s, z}, E_{\tau s}, E_{\tau, z s, z}) = \int_{A_k} (F_\tau F_s, F_{\tau, z} F_s, F_\tau F_{s, z}, F_{\tau, z} F_{s, z}) dz \quad (21)$$

where the subscript  $z$  indicates partial derivative with respect to  $z$ . Equation 20 becomes

$$\begin{aligned} & \int_{\Omega_k} \left[ (\mathbf{D}_p \delta \mathbf{u}_s^k)^T (E_{\tau s} \mathbf{C}_{pp}^k \mathbf{D}_p \mathbf{u}_\tau^k + E_{\tau s} \mathbf{C}_{pn}^k \mathbf{D}_{np} \mathbf{u}_\tau^k + E_{\tau, z s} \mathbf{C}_{pn}^k \mathbf{u}_\tau^k) \right. \\ & \quad + (\mathbf{D}_{np} \delta \mathbf{u}_s^k)^T (E_{\tau s} \mathbf{C}_{np}^k \mathbf{D}_p \mathbf{u}_\tau^k + E_{\tau s} \mathbf{C}_{nn}^k \mathbf{D}_{np} \mathbf{u}_\tau^k + E_{\tau, z s} \mathbf{C}_{nn}^k \mathbf{u}_\tau^k) \\ & \quad \left. + (\delta \mathbf{u}_s^k)^T (E_{\tau s, z} \mathbf{C}_{np}^k \mathbf{D}_p \mathbf{u}_\tau^k + E_{\tau s, z} \mathbf{C}_{nn}^k \mathbf{D}_{np} \mathbf{u}_\tau^k + E_{\tau, z s, z} \mathbf{C}_{nn}^k \mathbf{u}_\tau^k) \right] d\Omega_k = \delta L_e^k \end{aligned} \quad (22)$$

The integration by parts is required to obtain the strong form of the differential equations on  $\Omega_k$  and boundary conditions on  $\Gamma_k$ . Let us assume that  $\phi$  and  $\varphi$  are two generic columns of displacements or stresses, the integration by parts states

$$\int_{\Omega_k} (\mathbf{D}_\Omega \phi)^T \varphi d\Omega_k = - \int_{\Omega_k} \phi^T \mathbf{D}_\Omega^T \varphi d\Omega_k + \int_{\Gamma_k} \phi^T \mathbf{I}_\Omega \varphi d\Gamma_k \quad (23)$$

where  $\Omega = p, np$  and  $\mathbf{D}_\Omega$  denotes a generic array including only first order partial differential operators with respect to the in-plane coordinates  $x, y$ . The governing equations are

$$\delta \mathbf{u}_s^{k\tau} : \mathbf{K}_{uu}^{k\tau s} \mathbf{u}_\tau^k = \mathbf{P}_{u\tau}^k \quad (24)$$

and the boundary conditions are

$$\mathbf{\Pi}_{uu}^{k\tau s} u_\tau^k = \mathbf{\Pi}_{uu}^{k\tau s} \bar{u}_\tau^k \quad (25)$$

$\mathbf{P}_{u\tau}^k$  is the external load in Eq. 24. The fundamental nuclei,  $\mathbf{K}_{uu}^{k\tau s}$  and  $\mathbf{\Pi}_{uu}^{k\tau s}$ , are assembled through the depicted indexes,  $\tau$  and  $s$ , which consider the order of the expansion in  $z$  for the displacements. Superscript  $k$  denotes the assembly on the number of layers. The explicit form of the fundamental nuclei is

$$\begin{aligned} \mathbf{K}_{uu}^{k\tau s} = & (-\mathbf{D}_p^T) [\mathbf{C}_{pp}^k E_{\tau s} \mathbf{D}_p + \mathbf{C}_{pn}^k E_{\tau s} \mathbf{D}_{np} + \mathbf{C}_{pn}^k E_{\tau, z s}] \\ & - (\mathbf{D}_{np}^T) [\mathbf{C}_{pn}^k E_{\tau s} \mathbf{D}_p + \mathbf{C}_{nn}^k E_{\tau s} \mathbf{D}_{np} + \mathbf{C}_{nn}^k E_{\tau, z s}] \\ & + [\mathbf{C}_{np}^k E_{\tau s, z} \mathbf{D}_p + \mathbf{C}_{nn}^k E_{\tau s, z} \mathbf{D}_{np} + \mathbf{C}_{nn}^k E_{\tau, z s, z}] \end{aligned} \quad (26)$$

and for the boundary conditions

$$\begin{aligned} \mathbf{\Pi}_{uu}^{k\tau s} = & (I_p) [C_{pp}^k E_{\tau s} D_p + C_{np}^k E_{\tau s} D_{np} + C_{pn}^k E_{\tau, z s}] \\ & + (I_{np}) [C_{pn}^k E_{\tau s} D_p + C_{nn}^k E_{\tau s} D_{np} + C_{nn}^k E_{\tau, z s}] \end{aligned} \quad (27)$$

The following additional arrays have been introduced to perform the integration by parts:

$$\mathbf{I}_p = \begin{bmatrix} 1 & 0 & 0 \\ 0 & 1 & 0 \\ 1 & 1 & 0 \end{bmatrix} \quad (28)$$

$$\mathbf{I}_{np} = \begin{bmatrix} 0 & 0 & 1 \\ 0 & 0 & 1 \\ 0 & 0 & 0 \end{bmatrix} \quad (29)$$

## 2.4 Navier solution

In this paper the closed-form solution proposed by Navier for simply supported orthotropic plates is exploited. The following properties hold:

$$C_{pp16} = C_{pp26} = C_{pn63} = C_{pn36} = C_{nn45} = 0 \quad (30)$$

The terms  $\mathbf{u}_\tau^k$  are expressed as

$$\begin{aligned} u_{x_\tau}^k &= \sum_{m,n} \hat{U}_{x_\tau}^k \cdot \cos\left(\frac{m\pi x_k}{a_k}\right) \sin\left(\frac{n\pi y_k}{b_k}\right) & k = 1, N_l \\ u_{y_\tau}^k &= \sum_{m,n} \hat{U}_{y_\tau}^k \cdot \sin\left(\frac{m\pi x_k}{a_k}\right) \cos\left(\frac{n\pi y_k}{b_k}\right) & \tau = 1, N \\ u_{z_\tau}^k &= \sum_{m,n} \hat{U}_{z_\tau}^k \cdot \sin\left(\frac{m\pi x_k}{a_k}\right) \sin\left(\frac{n\pi y_k}{b_k}\right) \end{aligned} \quad (31)$$

where  $\hat{U}_{x_\tau}^k$ ,  $\hat{U}_{y_\tau}^k$  and  $\hat{U}_{z_\tau}^k$  are the amplitudes,  $m$  and  $n$  are the number of waves (they range from 0 to  $\infty$ ) and  $a_k$  and  $b_k$  are the dimensions of the plate. The final result is an algebraic equation system,

$$\delta \mathbf{u}_s^{k\tau} : \mathbf{K}_{uu}^{k\tau s} \mathbf{u}_\tau^k = \mathbf{P}_{u\tau}^k \quad (32)$$

Boundary conditions are exactly fulfilled by Eq. 31.

## 3 Method used to Evaluate the Effectiveness of Displacement Variables

The effectiveness of each higher-order term is evaluated through the mixed axiomatic/asymptotic method. This approach is based on the the following steps:

1. geometry, boundary conditions, materials and layer layouts are fixed;
2. a set of output parameters is chosen, such as displacement and stress components at a reference point;
3. the displacement variables to be analyzed are defined; in this paper all displacement variables of ED4 and LD4 models are analyzed;
4. a reference solution is defined; in the present work ED4 and LD4 approaches are adopted since the fourth order models offer an excellent agreement with the three-dimensional solutions as highlighted in [33];
5. CUF is used to generate the governing equations for the theories considered;
6. each displacement variable is deactivated in turn and its effectiveness is numerically established measuring the loss of accuracy compared with the reference solution;
7. any displacement variable which does not alter the mechanical response is considered not effective;
8. the most suitable structural model for a given structural problem is then obtained discarding the non-effective displacement variables.



A displacement variable is considered effective if its absence gives an error greater than 0.05% with respect to the reference solution, that is

$$\Delta = \left| 1 - \frac{Q}{Q_{\text{ref}}} \right| \times 100 > 0.05\% \quad (33)$$

where  $Q$  is a generic output (e.g. the transverse displacement in a point) and  $Q_{\text{ref}}$  is the reference value obtained through a full expansion model. A term of the expansion can be deactivated either by rearranging the rows and columns of the stiffness matrix or via a penalty technique. In this work a penalty technique was adopted. A graphic notation was introduced to represent the reduced models. Let us consider an LD4 model for an isotropic plate,

$$\begin{aligned} u_x &= F_t u_{xt} + F_2 u_{x2} + F_3 u_{x3} + F_4 u_{x4} + F_b u_{xb} \\ u_y &= F_t u_{yt} + F_2 u_{y2} + F_3 u_{y3} + F_4 u_{y4} + F_b u_{yb} \\ u_z &= F_t u_{zt} + F_2 u_{z2} + F_3 u_{z3} + F_4 u_{z4} + F_b u_{zb} \end{aligned} \quad (34)$$

If the term  $u_{z2}$  is suppressed the correspondent model is

$$\begin{aligned} u_x &= F_t u_{xt} + F_2 u_{x2} + F_3 u_{x3} + F_4 u_{x4} + F_b u_{xb} \\ u_y &= F_t u_{yt} + F_2 u_{y2} + F_3 u_{y3} + F_4 u_{y4} + F_b u_{yb} \\ u_z &= F_t u_{zt} + \quad + F_3 u_{z3} + F_4 u_{z4} + F_b u_{zb} \end{aligned} \quad (35)$$

In LW models the terms related with interfaces,  $\mathbf{u}_t$  and  $\mathbf{u}_b$ , can not be suppressed since this would introduce an extra constraint. The displacement field in Eq. 35 is given in Table 1. Table 2 explains the symbols adopted in Table 1.

In this work, different plates were considered; isotropic plates, orthotropic plates, cross-ply symmetric and unsymmetric composite plates and sandwich plates. Furthermore, the influence on the reduced model of the length-to-thickness ratio  $a/h$ , the orthotropic ratio  $E_L/E_T$ , the face-to-core Young's moduli ratio  $E_f/E_c$  and the stacking sequence was investigated.

## 4 Results

Results deal with simply supported square plates (unless otherwise indicated the side lengths are  $a = b = 0.1 \text{ m}$ ). The load is bisinusoidal and equal to

$$p = \bar{p}_z \cdot \sin\left(\frac{mx}{a}\right) \cdot \sin\left(\frac{ny}{b}\right) \quad (36)$$

where  $\bar{p}_z$  is equal to 1000 Pa.  $m$  and  $n$  are the numbers of waves along the two  $x$  and  $y$ , all analyses were carried out considering  $m = n = 1$ . Unless otherwise specified, the following outputs were evaluated:  $u_z$ ,  $\sigma_{xx}$  and  $\sigma_{zz}$  at  $[a/2 \ b/2 \ h/2]$ ,  $\sigma_{xz}$  at  $[0 \ b/2 \ 0]$  and  $\sigma_{yz}$  at  $[a/2 \ 0 \ 0]$ . The plate configuration is reported in Fig. 1.

### 4.1 Isotropic plates

Aluminum was considered,  $E = 73 \times 10^9 \text{ Pa}$  and  $\nu = 0.34$ . Two length-to-thickness ratios ( $a/h$ ) were considered, 100 (thin plate) and 2 (thick plate). In Table 3 results are reported from CLT, FSDT, ED4 and LD4 models. 3D analytical results were obtained as reported in [39], [40] and [41]. As well-known, refined models such as ED4 and LD4 are needed to properly detect transversal stresses  $\sigma_{xz}$ ,  $\sigma_{yz}$  and  $\sigma_{zz}$  and to analyze thick plates. CLT and FSDT models offer a good evaluation of displacement  $u_z$  and in-plane tension  $\sigma_{xx}$  for thin plates.

Table 3 shows that ED4 and LD4 are in good agreement with 3D results. For this reason, these models were chosen as references for the influence analysis of each displacement variable. Table 4 shows the influence of  $u_{z2}$  on the solution when deactivated. While transverse stresses  $\sigma_{xz}$  and  $\sigma_{yz}$  are not influenced, displacement  $u_z$  and in-plane stress  $\sigma_{xx}$  are affected. This means that  $u_{z2}$  must be considered to detect  $u_z$  and  $\sigma_{xx}$  whereas can be neglected to compute transversal stress. A similar analysis was carried out for an ED4 model but for the sake of brevity it has not been reported here (for more details see [33]). Through the analysis of Table 4, it is possible to create the ED4 and LD4 reduced models which

are reported in Table 5. Rows indicate the models considered (ED4, LD4) and the columns show the output variables considered. The ratio between the effective and total terms is reported ( $M_e$ ). The last column shows the reduced combined models, i.e. the models obtained considering the effective terms for all the output variables. For instance, the LD4 explicit reduced model for  $\sigma_{yz}$  of a thick plate ( $a/h = 2$ ) is ( $M_e = 9$ )

$$\begin{aligned} u_x &= F_t u_{xt} + F_3 u_{x3} + F_b u_{xb} \\ u_y &= F_t u_{yt} + F_3 u_{y3} + F_b u_{yb} \\ u_z &= F_t u_{zt} + F_4 u_{z4} + F_b u_{zb} \end{aligned} \quad (37)$$

In Figure 2 stresses  $\sigma_{xz}$  and  $\sigma_{zz}$  vs.  $z$  are reported; results were determined through ED4 and LD4 reduced models. The results obtained for the isotropic plate show that

1. although the reduced models were derived through the evaluation of variables on given points, the through-the-thickness behaviors are perfectly detected;
2. as the  $a/h$  decreases (thicker plates) the number of terms necessary to detect the solution increases, i.e. more unknown variables are needed;
3. full ED4 and LD4 models are required for thick plates ( $a/h = 2$ );
4. LD4 reduced models require more terms than ED4 models;
5. linear terms (i.e.  $u_{x2}$ ,  $u_{y2}$  and  $u_{z2}$ ) are crucial in the ESL reduced models;

## 4.2 Orthotropic plates

The influence of the orthotropic ratio, defined as  $E_L/E_T$ , on the accuracy of ED4 and LD4 reduced models is the subject of the next analyses. The plate properties are:  $E_T = E_z = 1 \times 10^9$  Pa, shear moduli are equal to  $0.39 \times 10^9$  Pa and Poisson's ratios are equal to 0.25. Young's modulus  $E_L$  is computed according to the orthotropic ratio  $E_L/E_T$ , assumed to be equal to 5 and 100. The  $a/h$  ratio influence is also considered. Table 6 shows the results obtained from the CLT, FSDT, ED4 and LD4 approaches. Data reported in the table show that a thick plate ( $a/h = 2$ ) can be better analyzed by means of ED4 or LD4. The influence of each displacement variable for various  $a/h$  and  $E_L/E_T$  ratios is carried out against LD4 and ED4 results since in [24] LD4 and ED4 effectiveness was proved. Table 7 reports the reduced models obtained for ED4 and LD4 models. In Figure 3,  $\sigma_{xz}$  and  $\sigma_{zz}$  vs  $z$  for ED4 and LD4 approaches are reported. The reported results suggest that:

1. although the reduced models were derived through the evaluation of variables on given points, the through-the-thickness behaviors are perfectly detected;
2. the length-to-thickness ratio and the orthotropic ratio influence the development of a reduced plate model, although the influence of  $a/h$  is stronger.

## 4.3 Composite plates

Composite plates are the subject of the next analyses. The composite plate considered for the axiomatic/asymptotic process has three layers of equal thickness. Each layer has properties of  $E_L = 40 \times 10^9$  Pa,  $E_T = E_z = 1 \times 10^9$  Pa,  $G_{LT} = 0.5 \times 10^9$  Pa,  $G_T = 0.6 \times 10^9$  Pa,  $\nu = 0.25$ . The orientation of the plies are :  $0^\circ/90^\circ/0^\circ$  and  $0^\circ/0^\circ/90^\circ$ . The results of the analysis of the static response are reported in Table 8. Three-dimensional exact elasticity results are obtained as reported in [40] and [41].

The influence of each displacement variable, as in the previous cases, was evaluated with respect to LD4 and ED4 models. In Figure 4 ED4 reduced model stresses are displayed,  $a/h$  is equal to 100 and the stacking sequence is  $0^\circ/90^\circ/0^\circ$ . Stresses  $\sigma_{xz}$  and  $\sigma_{yz}$  for the thick plate are reported in Figure 5. Plots referred to as FP-RM were defined through  $\sigma_{xz}$  and  $\sigma_{yz}$  reduced models built using single point values evaluated at  $z = 0$  (as in the previous analyses). It can be observed that the reduced model provides accurate results at  $z = 0$  but it is inaccurate elsewhere. Plots referred to as MP-RM were obtained using  $\sigma_{xz}$  and  $\sigma_{yz}$  reduced models based on maximum values. In this case the maximum values were at the interfaces between the top and the central layer. Reduced models built through MP-RM were able to detect correctly stresses through the entire thickness. In Tables 9 and 10 ED4 reduced models

are reported for fixed point and maximum point criteria. In some cases the reduced models coincide, as reported in Table 9. The reduced ED4 model for symmetric plates obtained through the MP-RM criterion is not reported since it is equivalent to the FP-RM reduced model. Reduced models for LD4 were also investigated. In Table 11 an example of displacement variable influence analysis is reported. Tables 12 and 13 report the LD4 reduced models for thin and thick plates, respectively. All analyses employed the maximum point criterion. In Figure 6 stresses along the thickness evaluated by means of LD4 reduced models are reported. It can be stated that

1. the maximum point criterion should be adopted to build the reduced models. This criterion, in fact, is able to detect the full model solution in proximity of the highest stress/displacement location;
2. asymmetric plates (e.g.  $0^\circ/0^\circ/90^\circ$ ) generally require more terms than symmetric plates;
3. the stacking sequence influences the development of a reduced model for both approaches.

#### 4.4 Sandwich plates

The analysis considers  $a/h$  equal to 4, 10, 100 and 1000. Differently from the previous cases the thickness is constantly equal to 0.01 m. All plates are square,  $a = b$ . Three different cases were considered. Benchmark 1 sandwich plate has two isotropic skins (aluminum, thickness  $h_1 = h_3 = 0.001$  m) and a Nomex core, its properties are  $E_L = E_T = 0.01 \times 10^6$  Pa,  $E_z = 75.85 \times 10^6$  Pa,  $G = 22.5 \times 10^6$ ,  $\nu = 0.25$ , thickness  $h_2 = 0.008$  m,  $E_f/E_c = 7.3 \times 10^6$ .  $E_f/E_c$  corresponds to the ratio of skin  $E_L$  value over the core  $E_L$  value. Benchmark 2 consists of two isotropic skins (aluminum,  $h_1 = h_2 = 0.001$  m) and a core which is 100 times less stiff than the core of benchmark 1, its properties are  $E_L = E_T = 0.0001 \times 10^6$  Pa,  $E_z = 0.7585 \times 10^6$  Pa,  $G = 0.225 \times 10^6$ ,  $\nu = 0.25$ , thickness  $h_2 = 0.008$  m,  $E_f/E_c = 7.3 \times 10^8$ . Benchmark 3 has 4 composite skins, their properties are  $E_L = 50 \times 10^9$  Pa,  $E_T = E_z = 10 \times 10^6$  Pa,  $G = 5 \times 10^9$  Pa,  $\nu = 0.25$ , thickness  $h_1 = h_2 = h_4 = h_5 = 0.0005$  m, the ply sequence is  $0^\circ/90^\circ - 90^\circ/0^\circ$ ,  $E_f/E_c = 50 \times 10^6$ . Its core is the same as in benchmark 1.

Table 14 reports the results of the benchmark 1 analysis. A good agreement was found between LD4 and 3D analytical results reported from [32]. For this reason LD4 was employed as reference model for the displacement variable effectiveness analysis. In Table 15, LD4 reduced models are reported for benchmark 1 and in Table 16 LD4 reduced models are reported for benchmark 2. In both cases the MP-RM criterion was applied. In Figure 7 stress  $\sigma_{xz}$  vs  $z$  obtained from LD4 reduced models is reported for thin and thick sandwich plates (benchmark 2). The maximum point criterion was adopted. The maximum value is correctly detected. In Table 17 LD4 reduced models are reported for  $a/h = 4$  and  $a/h = 100$  (benchmark 3). In Figure 7 the stress distribution over the thickness for benchmark 3 is reported, results were obtained via LD4 reduced models. In both cases the maximum value is correctly detected. It can be stated that

1. as for composite plates, the maximum point criterion should be used to develop reduced models.
2. the axiomatic/asymptotic method applied to the LW approach leads to a significant reduction of the total amount of unknown variables (some 50%) for sandwich plates.

## 5 Conclusion

This paper deals with the development of refined plate models for composite structure. Results were obtained through axiomatic/asymptotic analysis, allowing the development of reduced refined models through the analysis of the effectiveness of each displacement variable of a higher-order model. Terms not exhibiting influence on the solution were discarded in order to lower the amount of degrees of freedom. The Carrera Unified Formulation (CUF) was employed for the implementation of refined models and Navier - type closed solutions were considered for the analysis of simply-supported plates under a bisinusoidal transverse pressure. Equivalent Single Layer (ESL) and Layer Wise (LW) approaches were considered. The typology of considered plates included isotropic, orthotropic, composite and sandwich plates. The influence of specific parameters - length-to-thickness ratio  $a/h$ , orthotropic ratio  $E_L/E_T$ , skin-to-core Young's moduli ratio  $E_f/E_c$  and ply stacking sequence - were investigated. The analyses herein conducted make it possible to conclude that:

1. the set of effective terms can be strongly influenced by the displacement/stress component to be accounted for and by the geometrical and material characteristics;
2. although the reduced models were obtained through the evaluation of variables on given points, the displacement/stress components trend along the thickness is satisfactory;
3. the present methodology leads to significative reductions of the number of unknowns variables in a LW model. In layered and sandwich plates, a reduction of around 50% was obtained;
4. significative reductions were obtained for ESL models, although in some cases (thick plates) full ESL models had to be employed.

CUF theory has proved to be a versatile means to analyze different plates cases and to deal with a method that could be defined as a mixed axiomatic/asymptotic. In particular

1. CUF permits the evaluation of the accuracy of each problem variable by comparing the results with full refined models;
2. CUF makes it possible to consider the accuracy of the results as an input, and to detect the minimum set of variables required to fulfill the accuracy input.

Future investigations could consider improved reduction criteria in order to develop reduced models able to show more accurate displacement/stress trends along the thickness compared to a reference solution. In future shell geometries, dynamics, multifield problems, finite element analysis and nonlinear problems can be considered.

## References

- [1] L. Euler. *De curvis elasticis*. Lausanne and Geneva: Bousquet, 1744.
- [2] D. Bernoulli. *De vibrationibus et sono laminarum elasticarum, Commentarii Academiae Scientiarum Imperialis Petropolitanae*. Petropoli, 1751.
- [3] S. Timoshenko. On the correction for shear of the differential equation for transverse vibrations of prismatic bars. *Philosophical Magazine*, 41(6):744–746, 1921.
- [4] G. Kirchhoff. Über das gleichgewicht und die bewegung einer elastischen scheibe. *Journal fur reins und angewandte Mathematik*, 40:51–88, 1850. doi: 10.1515/crll.1850.40.51.
- [5] E. Reissner. The effect of transverse shear deformation on the bending of elastic plates. *Journal of Applied Mechanics*, 12:69–76, 1945. doi: 10.1515/crll.1850.40.51.
- [6] R. D. Mindlin. Influence of rotatory inertia and shear in flexural motions of isotropic elastic plates. *Journal of Applied Mechanics*, 18:1031–1036, 1950. doi: 10.1515/crll.1850.40.51.
- [7] S. A. Ambartsumian. Contributions to the theory of anisotropic layered shells. *Applied Mechanics Reviews*, 15(4), 1962.
- [8] L. Librescu and J.N. Reddy. *A critical Review and Generalization of Transverse Shear Deformable Anisotropic Plates, Euromech Colloquium 219, Kassel. Refined Dynamical Theories of Beams, Plates and Shells and Their Applications*. I. Elishakoff and H. Irretier, Springer-Verlag, Berlin, 1986.
- [9] E. I. Grigolyuk and G. M. Kulikov. General directions of the development of theory of shells. *Mechanics of Composite Materials*, 24(2):231–241, 1988. doi: 10.1515/crll.1850.40.51.
- [10] A. K. Noor and W. S. Burton. Assessment of shear deformation theories for multilayered composite plates. *Applied Mechanics Reviews*, 42(1):1–18, 1989. doi: 10.1115/1.3152418.
- [11] P. Cicala. *Systematic Approximation Approach to Linear Shell Theory*. Levrotto e Bella, Torino, 1965.

- [12] A. L. Gol'denweizer. *Theory of Thin Elastic Shells, International Series of Monograph in Aeronautics and Astronautics*. Pergamon, New York, 1961.
- [13] P. Cicala. Sulla teoria elastica della parete sottile. *Giornale del genio civile*, 4, 6, 9:1026–1037, 1959.
- [14] W. Yu and D. H. Hodges. Generalized timoshenko theory of the variational asymptotic beam sectional analysis. *Journal of the American Helicopter Society*, 50(1):46–55, 2005. doi: 10.4050/1.3092842.
- [15] O. A. Fettahlioglu and C. R. Steele. Asymptotic solutions for orthotropic nonhomogeneous shells of revolution. *Journal of Applied Mechanics*, 41(3):753–758, 1974. doi: 10.1115/1.3423383.
- [16] V. L. Berdichevsky. Variational-asymptotic method of shell theory construction. *Prikladnaya Matematika i Mekhanika*, 43:664–667, 1979.
- [17] V. L. Berdichevsky and V. Misyura. Effect of accuracy loss in classical shell theory. *Journal of Applied Mechanics*, 59(2):s217–s223, 1992. doi: 10.1115/1.2899492.
- [18] J. N. Reddy. *Mechanics of Laminated Plates, Theory and Analysis*. CRC Press, Boca Raton, 1997.
- [19] A. R. Setoodeha and G. Karamib. Static, free vibration and buckling analysis of anisotropic thick laminated composite plates on distributed and point elastic supports using a 3-d layer-wise fem. *Engineering Structures*, 26:211–220, 2004. [http://dx.note.org/10.1016/0020-7683\(91\)90200-Y](http://dx.note.org/10.1016/0020-7683(91)90200-Y).
- [20] C. M. C. Roque, A. J. M. Ferreira, and R. M. N. Jorge. Free vibration analysis of composite and sandwich plates by a trigonometric layerwise deformation theory and radial basis functions. *Journal of Sandwich Structures and Materials*, 8:497–515, 2006.
- [21] A. J. M. Ferreira. Analysis of composite plates using a layerwise theory and multiquadrics discretization. *Mechanics of Advanced Materials and Structures*, 12:99–112, 2005.
- [22] J. N. Reddy and E. J. Barbero. Modeling of delamination in composite laminates using a layer-wise plate theory. *International Journal of Solids and Structures*, 28:373–388, 1991. [http://dx.note.org/10.1016/0020-7683\(91\)90200-Y](http://dx.note.org/10.1016/0020-7683(91)90200-Y).
- [23] S. S. Phoenix, S. K. Satsangia, and B.N. Singhb. Layer-wise modeling of magneto-electro-elastic plates. *Journal of Sound and Vibration*, 324:798–815, 2009. [http://dx.note.org/10.1016/0020-7683\(91\)90200-Y](http://dx.note.org/10.1016/0020-7683(91)90200-Y).
- [24] E. Carrera. Theories and finite elements for multilayered plates and shells: A unified compact formulation with numerical assessment and benchmarking. *Arch. Comput. Meth. Engng*, 10(3):215–296, 2003.
- [25] E. Carrera, S. Brischetto, and P. Nali. *Plates and Shells for Smart Structures Classical and Advanced Theories for Modeling and Analysis*. Wiley, New Delhi, 2011.
- [26] E. Carrera, G. Giunta, and M. Petrolo. *Beam Structures, Classical and Advanced Theories*. Wiley, New Delhi, 2011.
- [27] E. Carrera. Evaluation of Layer-Wise Mixed Theories for Laminated Plates Analysis. *AIAA Journal*, 36(5):830–839, 1998. doi: 10.2514/2.444
- [28] E. Carrera. Layer-Wise Mixed Models for Accurate Vibration Analysis of Multilayered Plates. *Journal of Applied Mechanics*, 65(4):820–828, 1998. doi: 10.1115/1.2791917
- [29] E. Carrera and A. Ciuffreda. Bending of composites and sandwich plates subjected to localized lateral loadings: a comparison of various theories. *Composite Structures*, 68(2):185–202, 2005. doi: 10.1016/j.compstruct.2004.03.013
- [30] M. Boscolo. Analytical solution for free vibration analysis of composite plates with layer-wise displacement assumptions. *Composite Structures*, 100:493 – 510, 2013. <http://dx.doi.org/10.1016/j.compstruct.2013.01.015>.

- [31] E. Carrera, P. Nali, and S. Lecca. Assessments of refined theories for buckling analysis of laminated plates. *Composite Structures*, 93(2):456 – 464, 2011. <http://dx.doi.org/10.1016/j.compstruct.2010.08.035>.
- [32] E. Carrera and S. Brischetto. A survey with numerical assessment of classical and refined theories for the analysis of sandwich plates. *Applied Mechanics Reviews*, 62:1–17, 2009. doi: 10.1115/1.3013824.
- [33] E. Carrera and M. Petrolo. Guidelines and recommendation to construct theories for metallic and composite plates. *AIAA Journal*, 48(12):2852–2866, 2010. doi: 10.2514/1.J050316.
- [34] E. Carrera and M. Petrolo. On the effectiveness of higher-order terms in refined beam theories. *Journal of Applied Mechanics*, 78(2), 2011.
- [35] E. Carrera, F. Miglioretti, and M. Petrolo. Accuracy of refined finite elements for laminated plate analysis. *Composite Structures*, 93(5):1311–1327, 2011. doi: 10.1016/j.compstruct.2010.11.007.
- [36] E. Carrera, F. Miglioretti, and M. Petrolo. Guidelines and recommendations on the use of higher orderfinite elements for bending analysis of plates. *International Journal for Computational Methods in Engineering Science and Mechanics*, 12, 2011.
- [37] E. Carrera, F. Miglioretti, and M. Petrolo. Computations and evaluations of higher-order theories for free vibration analysis of beams. *Journal of Sound and Vibration*, 331, 2012.
- [38] S. W. Tsai. *Composites Design, 4th ed.* Think Composites, Dayton, 1988.
- [39] E. Carrera, G. Giunta, and S. Belouettar. A refined beam theory with only displacement variables and deformable cross-section. In *50th AIAA/ASME/ASCE/AHS/ASC Structures, Structural Dynamics, and Materials Conference*, Palm Springs, CA, 4-7 May 2009.
- [40] E. Carrera, G. Giunta, and S. Brischetto. Hierarchical closed form solutions for plates bent by localized transverse loadings. *Journal of Zhejiang University Science B*, 8(7):1026–1037, 2007. doi:10.1631/jzus.2007.A1026.
- [41] E. Carrera and G. Giunta. Hierarchical models for failure analysis of plates bent by distributed and localized transverse loadings. *Journal of Zhejiang University Science A*, 9(5):600–613, 2008. doi:10.1631/jzus.A072110.

## Table Caption List

1. Table 1: Reduced LW plate model with  $u_{z2}$  deactivated.
2. Table 2: Symbols adopted to indicate the status of a displacement variable.
3. Table 3: Isotropic square plate.  $\bar{u}_z = u_z E_T h^3 / (\bar{p}_z a^4)$ .  $(\bar{\sigma}_{xx}, \bar{\sigma}_{yz}, \bar{\sigma}_{zz}) = (\sigma_{xx}, \sigma_{yz}, \sigma_{zz}) / (p_z (a/h))$ .
4. Table 4: Isotropic plate, influence of each displacement variable on the solution. LD4 approach,  $a/h = 100$ .
5. Table 5: Summary of the effective terms for the isotropic plate with different  $a/h$  ratios. ED4 and LD4 approaches.
6. Table 6: Orthotropic square plate displacements and stresses.
7. Table 7: Summary of the effective terms for the orthotropic plate with different  $E_L/E_T$  ratios. ED4 and LD4 approaches.
8. Table 8: Composite square plate displacements and stresses.
9. Table 9: Summary of the effective terms for the composite plate with different ply orientations. ED4 approach,  $a/h = 100$ . Maximum (MP) and fixed point (FP) criteria.

10. Table 10: Summary of the effective terms for the composite plate with different ply orientations. ED4 approach,  $a/h = 2$ . Maximum (MP) and fixed point (FP) criteria.
11. Table 11: Influence of each displacement variable, composite plate. Maximum point criterium. Ply sequence:  $0^\circ/0^\circ/90^\circ$ ,  $a/h = 100$ .
12. Table 12: Summary of the effective terms for the composite plate with different layers orientation. LD4 approach,  $a/h = 100$ . Maximum point criterium.
13. Table 13: Summary of the effective terms for the composite plate with different layers orientation. LD4 approach,  $a/h = 2$ . Maximum point criterium.
14. Table 14: Sandwich plate, benchmark 1.  $(\bar{\sigma}_{xx}, \bar{\sigma}_{xz}) = (\sigma_{xx}, \sigma_{xz})/p_z$ .
15. Table 15: Reduced models for a sandwich plate, benchmark 1. LD4 approach,  $a/h = 4$  and  $a/h = 100$ .
16. Table 16: Reduced models for a sandwich plate, benchmark 2. LD4 approach,  $a/h = 4$  and  $a/h = 100$ .
17. Table 17: Reduced model for sandwich plates, benchmark 3.

## Figure Caption List

1. Figure 1: Plate reference frame.
2. Figure 2:  $\bar{\sigma}_{yz}$  and  $\bar{\sigma}_{zz}$  vs  $z$ . Isotropic plate,  $a/h = 100$ . RM stands for reduced model.
  - Figure 2a:  $\bar{\sigma}_{yz}$ .
  - Figure 2b:  $\bar{\sigma}_{zz}$ .
3. Figure 3:  $\bar{\sigma}_{yz}$  and  $\bar{\sigma}_{zz}$  vs  $z$ . Orthotropic plate.  $a/h = 100$ ,  $E_L/E_T = 100$ .
  - Figure 3a:  $\bar{\sigma}_{yz}$ .
  - Figure 3b:  $\bar{\sigma}_{zz}$ .
4. Figure 4:  $\bar{\sigma}_{xz}$  and  $\bar{\sigma}_{yz}$  vs  $z$ . Composite plate,  $a/h = 100$ , ply sequence:  $0^\circ/90^\circ/0^\circ$ . Fixed point criterium.
  - Figure 4a:  $\bar{\sigma}_{xz}$ .
  - Figure 4b:  $\bar{\sigma}_{yz}$ .
5. Figure 5:  $\bar{\sigma}_{xz}$  and  $\bar{\sigma}_{yz}$  vs  $z$ . Composite plate,  $a/h = 2$ .
  - Figure 5a:  $\bar{\sigma}_{xz}$ . Ply sequence:  $0^\circ/90^\circ/0^\circ$ .
  - Figure 5b:  $\bar{\sigma}_{yz}$ . Ply sequence:  $0^\circ/0^\circ/90^\circ$ .
6. Figure 6:  $\bar{\sigma}_{xz}$  and  $\bar{\sigma}_{yz}$  vs  $z$ . Composite plate,  $a/h = 100$ . Maximum point criterium.
  - Figure 6a:  $\bar{\sigma}_{yz}$ . Ply sequence:  $0^\circ/90^\circ/0^\circ$ .
  - Figure 6b:  $\bar{\sigma}_{xz}$ . Ply sequence:  $0^\circ/0^\circ/90^\circ$ .
7. Figure 7: Sandwich benchmarks 2 and 3, reduced combined models. Maximum point criterium.
  - Figure 7a: Sandwich plate benchmark 2.  $a/h = 4$ .
  - Figure 7b: Sandwich plate benchmark 2.  $a/h = 100$ .
  - Figure 7c: Sandwich plate benchmark 3.  $a/h = 4$ .
  - Figure 7d: Sandwich plate benchmark 3.  $a/h = 100$ .

## Tables

■	▲	▲	▲	■
■	▲	▲	▲	■
■	△	▲	▲	■

Table 1: Reduced LW plate model with  $u_{z2}$  deactivated

Active term	Inactive term	Non-deactivable term
▲	△	■

Table 2: Symbols adopted to indicate the status of a displacement variable.

a/h		$\bar{u}_z$	$\bar{\sigma}_{xx}$	$\bar{\sigma}_{yz}$	$\bar{\sigma}_{zz}$
100	3D	2.7248	0.2037	0.2387	0.0100
	CLT	2.7237	0.2037	0.1592	21.3150
	FSDT	2.7251	0.2037	0.1592	21.3150
	ED4	2.7248	0.2037	0.2387	0.0100
	LD4	2.7248	0.2037	0.2387	0.0100
2	3D	7.3826	0.3145	0.2277	0.5000
	CLT	2.7238	0.2037	0.1592	0.4263
	FSDT	6.1178	0.2037	0.1592	0.4263
	ED4	7.3811	0.3165	0.2306	0.5082
	LD4	7.3811	0.3165	0.2306	0.5082

Table 3: Isotropic square plate.  $\bar{u}_z = u_z E_T h^3 / (\bar{p}_z a^4)$ .  $(\bar{\sigma}_{xx}, \bar{\sigma}_{yz}, \bar{\sigma}_{zz}) = (\sigma_{xx}, \sigma_{yz}, \sigma_{zz}) / (p_z (a/h))$

	$u_z$	$\sigma_{xx}$	$\sigma_{xz}$	$\sigma_{yz}$	$\sigma_{zz}$															
<table><tr><td>■</td><td>▲</td><td>▲</td><td>▲</td><td>■</td></tr><tr><td>■</td><td>▲</td><td>▲</td><td>▲</td><td>■</td></tr><tr><td>■</td><td>△</td><td>▲</td><td>▲</td><td>■</td></tr></table>	■	▲	▲	▲	■	■	▲	▲	▲	■	■	△	▲	▲	■	73.49	113.07	100.00	100.00	$0.157 \times 10^6$
■	▲	▲	▲	■																
■	▲	▲	▲	■																
■	△	▲	▲	■																

Table 4: Isotropic plate, influence of each displacement variable on the solution. LD4 approach,  $a/h = 100$ .

$u_z$ 
 $\sigma_{xx}$ 
 $\sigma_{xz}$ 
 $\sigma_{yz}$ 
 $\sigma_{zz}$ 
COMBINED

a/h=100

$M_e = 4/15$   

△	▲	△	△	△
△	▲	△	△	△
△	▲	△	△	△

$M_e = 4/15$   

△	▲	△	△	△
△	▲	△	△	△
△	▲	△	△	△

$M_e = 5/15$   

△	▲	△	▲	△
△	▲	△	▲	△
△	▲	△	▲	△

$M_e = 5/15$   

△	▲	△	△	△
△	▲	△	▲	△
△	▲	△	△	△

$M_e = 4/15$   

△	△	△	△	△
△	△	△	△	△
△	△	△	△	△

$M_e = 8/15$   

△	▲	△	▲	△
△	▲	△	▲	△
△	▲	△	▲	△

$M_e = 7/15$   

■	△	△	△	■
■	△	△	△	■
■	△	△	△	■

$M_e = 7/15$   

■	△	△	△	■
■	△	△	△	■
■	△	△	△	■

$M_e = 7/15$   

■	△	▲	△	■
■	△	▲	△	■
■	△	▲	△	■

$M_e = 7/15$   

■	△	△	△	■
■	△	▲	△	■
■	△	△	△	■

$M_e = 8/15$   

■	△	△	△	■
■	△	△	△	■
■	△	△	△	■

$M_e = 10/15$   

■	△	▲	△	■
■	△	▲	△	■
■	△	▲	△	■

a/h=2

$M_e = 13/15$   

▲	▲	▲	▲	△
▲	▲	▲	▲	△
▲	▲	▲	▲	△

$M_e = 14/15$   

▲	▲	△	▲	▲
▲	▲	△	▲	▲
▲	▲	△	▲	▲

$M_e = 7/15$   

△	▲	△	▲	△
△	▲	△	▲	△
△	▲	△	▲	△

$M_e = 7/15$   

△	▲	△	▲	△
△	▲	△	▲	△
△	▲	△	▲	△

$M_e = 13/15$   

▲	△	▲	▲	▲
▲	△	▲	▲	▲
▲	△	▲	▲	▲

$M_e = 15/15$   

▲	▲	▲	▲	▲
▲	▲	▲	▲	▲
▲	▲	▲	▲	▲

$M_e = 12/15$   

■	▲	▲	△	■
■	▲	▲	△	■
■	△	▲	▲	■

$M_e = 15/15$   

■	▲	▲	▲	■
■	▲	▲	▲	■
■	▲	▲	▲	■

$M_e = 9/15$   

■	△	▲	△	■
■	△	▲	△	■
■	△	△	▲	■

$M_e = 9/15$   

■	△	▲	△	■
■	△	△	▲	■
■	△	△	▲	■

$M_e = 15/15$   

■	▲	▲	▲	■
■	▲	▲	▲	■
■	▲	▲	▲	■

$M_e = 15/15$   

■	▲	▲	▲	■
■	▲	▲	▲	■
■	▲	▲	▲	■

Table 5: Summary of the effective terms for the isotropic plate with different a/h ratios. ED4 and LD4 approaches.



$E_L/E_T$		$\bar{u}_z$	$\bar{\sigma}_{xx}$	$\bar{\sigma}_{xz}$	$\bar{\sigma}_{yz}$	$\bar{\sigma}_{zz}$
		a/h=100				
5	CLT	1.5130	0.3969	0.2383	0.0800	4.7372
	FSDT	1.5146	0.3969	0.2383	0.0800	4.7381
	ED4	1.5148	0.3970	0.3574	0.1200	0.0100
	LD4	1.5148	0.3970	0.3574	0.1200	0.0100
100	CLT	0.1195	0.5914	0.3120	0.0063	0.3547
	FSDT	0.1220	0.5911	0.3120	0.0064	0.3578
	ED4	0.1224	0.5936	0.4676	0.0096	0.0100
	LD4	0.1224	0.5936	0.4676	0.0096	0.0100
		a/h=2				
5	CLT	1.5130	0.3970	0.2383	0.0780	0.0947
	FSDT	5.1754	0.3078	0.2000	0.1183	0.1162
	ED4	7.3829	0.5750	0.2669	0.1798	0.5073
	LD4	7.3829	0.5750	0.2669	0.1798	0.5073
100	CLT	0.1195	0.5914	0.3120	0.0063	0.0071
	FSDT	4.6031	0.3722	0.2222	0.0961	0.0721
	ED4	6.5436	1.6629	0.2297	0.1440	0.5053
	LD4	6.5436	1.6629	0.2297	0.1440	0.5053

Table 6: Orthotropic square plate displacements and stresses.








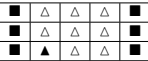
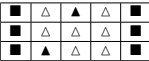










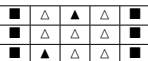









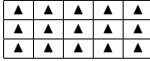
















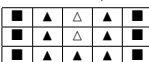






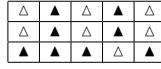
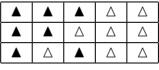



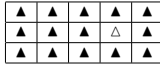
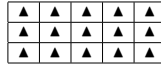
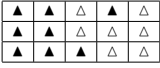

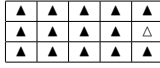
	$u_z$	$\sigma_{xx}$	$\sigma_{xz}$	$\sigma_{yz}$	$\sigma_{zz}$	COMBINED
$a/h=100$						
$E_L/E_T=5$						
ED4	$M_e = 4/15$ 	$M_e = 4/15$ 	$M_e = 5/15$ 	$M_e = 5/15$ 	$M_e = 4/15$ 	$M_e = 8/15$ 
LD4	$M_e = 7/15$ 	$M_e = 7/15$ 	$M_e = 8/15$ 	$M_e = 8/15$ 	$M_e = 8/15$ 	$M_e = 10/15$ 
$E_L/E_T=100$						
ED4	$M_e = 4/15$ 	$M_e = 5/15$ 	$M_e = 4/15$ 	$M_e = 6/15$ 	$M_e = 4/15$ 	$M_e = 8/15$ 
LD4	$M_e = 8/15$ 	$M_e = 8/15$ 	$M_e = 8/15$ 	$M_e = 9/15$ 	$M_e = 8/15$ 	$M_e = 10/15$ 
$a/h=2$						
$E_L/E_T=5$						
ED4	$M_e = 11/15$ 	$M_e = 15/15$ 	$M_e = 7/15$ 	$M_e = 7/15$ 	$M_e = 12/15$ 	$M_e = 15/15$ 
LD4	$M_e = 13/15$ 	$M_e = 15/15$ 	$M_e = 10/15$ 	$M_e = 10/15$ 	$M_e = 14/15$ 	$M_e = 15/15$ 
$E_L/E_T=100$						
ED4	$M_e = 12/15$ 	$M_e = 13/15$ 	$M_e = 7/15$ 	$M_e = 6/15$ 	$M_e = 10/15$ 	$M_e = 15/15$ 
LD4	$M_e = 13/15$ 	$M_e = 13/15$ 	$M_e = 10/15$ 	$M_e = 10/15$ 	$M_e = 13/15$ 	$M_e = 15/15$ 

Table 7: Summary of the effective terms for the orthotropic plate with different  $E_L/E_T$  ratios. ED4 and LD4 approaches.

	$\bar{u}_z$	$\bar{\sigma}_{xx}$	$\bar{\sigma}_{xz}$	$\bar{\sigma}_{yz}$	$\bar{\sigma}_{zz}$
a/h=100					
0°/90°/0°					
CLT	0.2836	0.5637	0.3280	0.0239	0.8448
FSDT	0.2852	0.5634	0.3279	0.0240	0.8465
ED4	0.2854	0.5639	0.4542	0.0449	0.0100
LD4	0.2854	0.5639	0.4054	0.0727	0.0100
0°/0°/90°					
CLT	0.6534	0.0461	0.2190	0.0900	1.5714
FSDT	0.6546	0.0461	0.2189	0.0901	1.5714
ED4	0.6553	0.0463	0.3477	0.1089	0.0485
LD4	0.6553	0.0462	0.3867	0.0912	0.0100
a/h=2					
0°/90°/0°					
CLT	0.2828	0.5625	0.3277	0.0238	0.0169
FSDT	3.1598	0.3536	0.2255	0.1040	0.0456
ED4	5.3692	1.2074	0.2687	0.1632	0.5091
LD4	5.5094	1.4089	0.2541	0.2000	0.5025
0°/0°/90°					
CLT	0.6515	0.0460	0.2188	0.0900	0.0314
FSDT	3.1153	0.0375	0.1657	0.1499	0.0319
ED4	5.7526	0.2015	0.2140	0.1914	0.5062
LD4	5.8611	0.2065	0.2313	0.1741	0.5021

Table 8: Composite square plate displacements and stresses

	$u_z$	$\sigma_{xx}$	$\sigma_{xz}$	$\sigma_{yz}$	$\sigma_{zz}$	COMBINED
0°/90°/0°						
FP	$M_e = 5/15$	$M_e = 5/15$	$M_e = 5/15$	$M_e = 6/15$	$M_e = 7/15$	$M_e = 8/15$
						
0°/0°/90°						
FP	$M_e = 7/15$	$M_e = 10/15$	$M_e = 10/15$	$M_e = 10/15$	$M_e = 14/15$	$M_e = 15/15$
						
MP	—*	$M_e = 8/15$	—	$M_e = 11/15$	$M_e = 14/15$	—
	—*		—			—

(\*): in this case the MP model coincides with the FP model.

Table 9: Summary of the effective terms for the composite plate with different ply orientations. ED4 approach,  $a/h = 100$ . Maximum (MP) and fixed point (FP) criteria.

	$u_z$	$\sigma_{xx}$	$\sigma_{xz}$	$\sigma_{yz}$	$\sigma_{zz}$	COMBINED
$0^\circ/90^\circ/0^\circ$						
FP	$M_e = 11/15$ 	$M_e = 13/15$ 	$M_e = 7/15$ 	$M_e = 7/15$ 	$M_e = 13/15$ 	$M_e = 15/15$ 
MP	—*	—	$M_e = 12/15$ 	$M_e = 13/15$ 	—	—
$0^\circ/0^\circ/90^\circ$						
FP	$M_e = 14/15$ 	$M_e = 15/15$ 	$M_e = 14/15$ 	$M_e = 14/15$ 	$M_e = 15/15$ 	$M_e = 15/15$ 
MP	—	$M_e = 14/15$ 	$M_e = 15/15$ 	$M_e = 15/15$ 	—	—

(\*): in this case the MP model coincides with the FP model.

Table 10: Summary of the effective terms for the composite plate with different ply orientations. ED4 approach,  $a/h = 2$ . Maximum (MP) and fixed point (FP) criteria.

	$u_z$	$\sigma_{xx}$	$\sigma_{xz}$	$\sigma_{yz}$	$\sigma_{zz}$
	99.93	99.93	99.93	100.23	6587.50

Table 11: Influence of each displacement variable, composite plate. Maximum point criterium. Ply sequence:  $0^\circ/0^\circ/90^\circ$ ,  $a/h = 100$ .

	$0^\circ/90^\circ/0^\circ$	$0^\circ/0^\circ/90^\circ$
	$M_e = 12/39$	$M_e = 15/39$
$u_z$		
	$M_e = 14/39$	$M_e = 15/39$
$\sigma_{xx}$		
	$M_e = 13/39$	$M_e = 17/39$
$\sigma_{xz}$		
	$M_e = 14/39$	$M_e = 17/39$
$\sigma_{yz}$		
	$M_e = 15/39$	$M_e = 15/39$
$\sigma_{zz}$		
COMBINED	$M_e = 20/39$	$M_e = 21/39$

Table 12: Summary of the effective terms for the composite plate with different layers orientation. LD4 approach,  $a/h = 100$ . Maximum point criterium

	$0^\circ/90^\circ/0^\circ$	$0^\circ/0^\circ/90^\circ$
	$M_e = 24/39$	$M_e = 24/39$
$u_z$		
	$M_e = 26/39$	$M_e = 28/39$
$\sigma_{xx}$		
	$M_e = 24/39$	$M_e = 23/39$
$\sigma_{xz}$		
	$M_e = 27/39$	$M_e = 24/39$
$\sigma_{yz}$		
	$M_e = 17/39$	$M_e = 17/39$
$\sigma_{zz}$		
COMBINED	$M_e = 29/39$	$M_e = 30/39$

Table 13: Summary of the effective terms for the composite plate with different layers orientation. LD4 approach,  $a/h = 2$ . Maximum point criterium

	$\bar{u}_z$	$\bar{\sigma}_{xx}$	$\bar{\sigma}_{xz}$
a/h=100			
3D	7.1881	4288.00	17.594
CLT	5.5798	4172.00	0.0655
FSDT	5.5866	4172.00	0.0655
ED1	5.5866	4172.70	0.0655
ED2	5.5896	4171.50	0.0711
ED3	5.7497	4178.40	2.4241
ED4	5.7498	4192.60	2.4239
LD1	7.1743	4568.90	17.5580
LD2	7.1880	4288.00	17.5910
LD3	7.1880	4287.90	17.5940
LD4	7.1880	4287.90	17.5940
a/h=4			
3D	590.54	67.958	0.4053
CLT	5.5799	6.6752	0.0026
FSDT	9.8085	6.6752	0.0026
ED1	9.8085	7.2882	0.0026
ED2	10.0666	7.2266	0.0028
ED3	100.8494	12.8060	0.0882
ED4	101.7211	6.2903	0.0896
LD1	506.2226	88.1830	0.3509
LD2	590.4421	67.9520	0.4085
LD3	590.5365	67.9860	0.4053
LD4	590.5340	67.9580	0.4053

Table 14: Sandwich plate, benchmark 1.  $(\bar{\sigma}_{xx}, \bar{\sigma}_{xz}) = (\sigma_{xx}, \sigma_{xz})/p_z$













	$a/h = 100$	$a/h = 4$
	$M_e = 14/39$	$M_e = 15/39$
$u_z$		
	$M_e = 14/39$	$M_e = 15/39$
$\sigma_{xx}$		
	$M_e = 14/39$	$M_e = 16/39$
$\sigma_{xz}$		
	$M_e = 14/39$	$M_e = 16/39$
$\sigma_{yz}$		
	$M_e = 15/39$	$M_e = 15/39$
$\sigma_{zz}$		
	$M_e = 16/39$	$M_e = 19/39$
COMBINED		

Table 15: Reduced models for a sandwich plate, benchmark 1. LD4 approach,  $a/h = 4$  and  $a/h = 100$ .

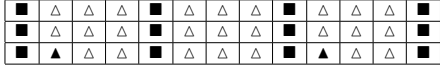
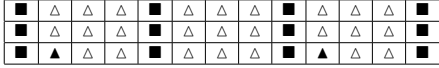
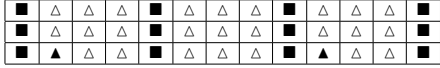
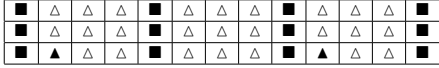

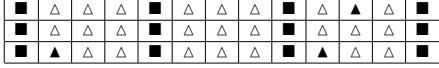

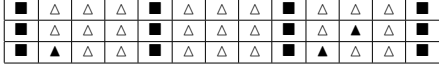

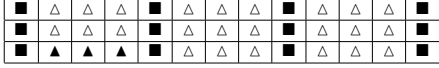
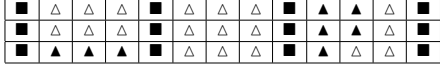
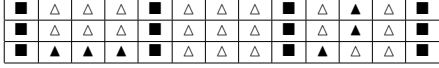
	$a/h = 100$	$a/h = 4$
	$M_e = 14/39$	$M_e = 14/39$
$u_z$		
	$M_e = 14/39$	$M_e = 14/39$
$\sigma_{xx}$		
	$M_e = 16/39$	$M_e = 15/39$
$\sigma_{xz}$		
	$M_e = 16/39$	$M_e = 15/39$
$\sigma_{yz}$		
	$M_e = 15/39$	$M_e = 15/39$
$\sigma_{zz}$		
	$M_e = 20/39$	$M_e = 18/39$
COMBINED		

Table 16: Reduced models for a sandwich plate, benchmark 2. LD4 approach,  $a/h = 4$  and  $a/h = 100$ .

Table 17: Reduced model for sandwich plates, benchmark 3.



# Figures

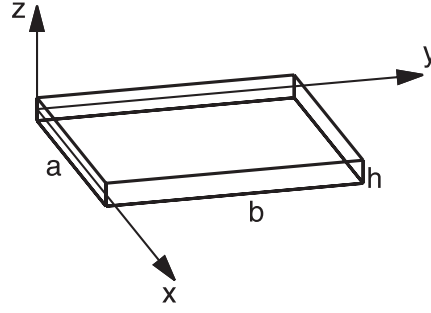


Figure 1: Plate reference frame.

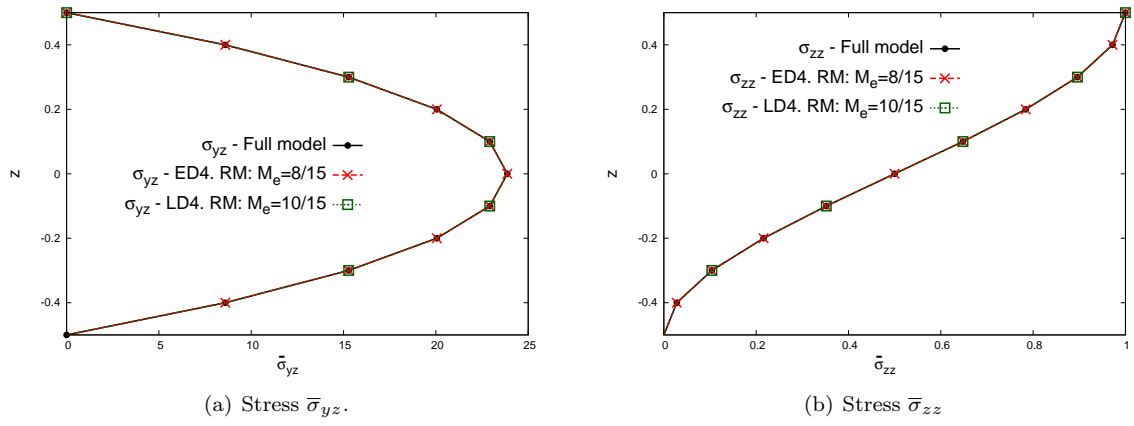


Figure 2:  $\bar{\sigma}_{yz}$  and  $\bar{\sigma}_{zz}$  vs  $z$ . Isotropic plate,  $a/h = 100$ . RM stands for reduced model.

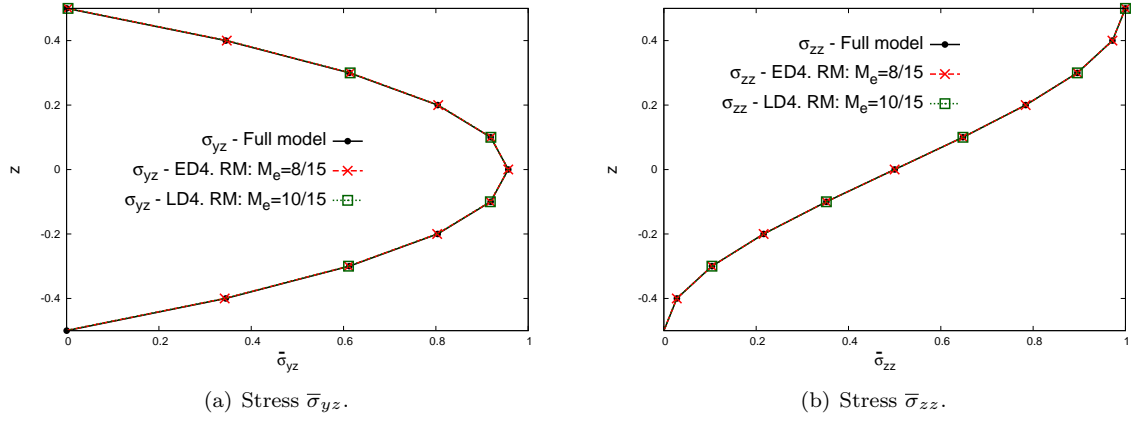
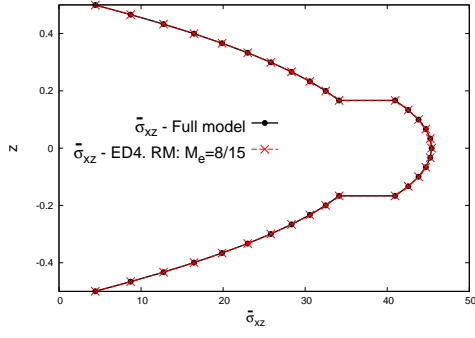
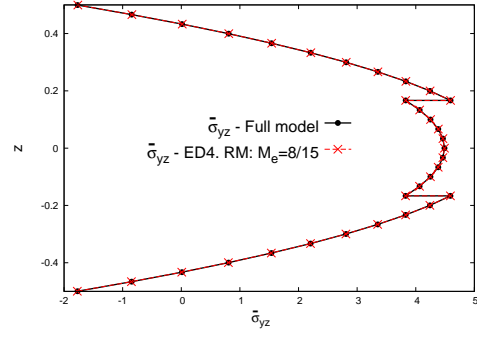


Figure 3:  $\bar{\sigma}_{yz}$  and  $\bar{\sigma}_{zz}$  vs  $z$ . Orthotropic plate.  $a/h = 100$ ,  $E_L/E_T = 100$ .

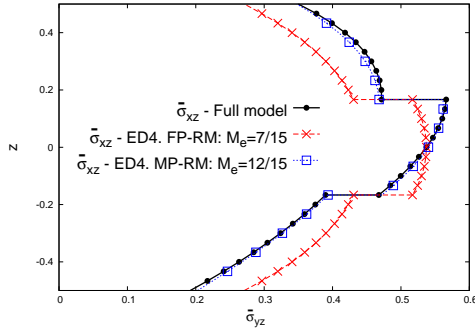


(a) Stress  $\bar{\sigma}_{xz}$ .

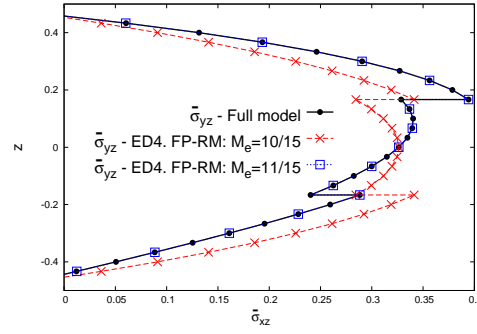


(b) Stress  $\bar{\sigma}_{yz}$ .

Figure 4:  $\bar{\sigma}_{xz}$  and  $\bar{\sigma}_{yz}$  vs  $z$ . Composite plate,  $a/h = 100$ , ply sequence:  $0^\circ/90^\circ/0^\circ$ . Fixed point criterium.

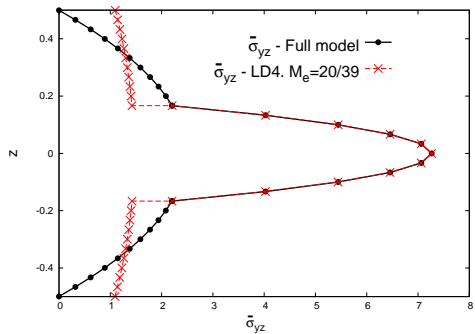


(a) Stress  $\bar{\sigma}_{xz}$ . Ply sequence:  $0^\circ/90^\circ/0^\circ$ .

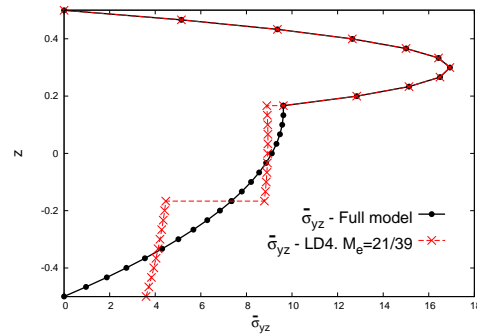


(b) Stress  $\bar{\sigma}_{yz}$ . Ply sequence:  $0^\circ/0^\circ/90^\circ$ .

Figure 5:  $\bar{\sigma}_{xz}$  and  $\bar{\sigma}_{yz}$  vs  $z$ . Composite plate,  $a/h = 2$ .

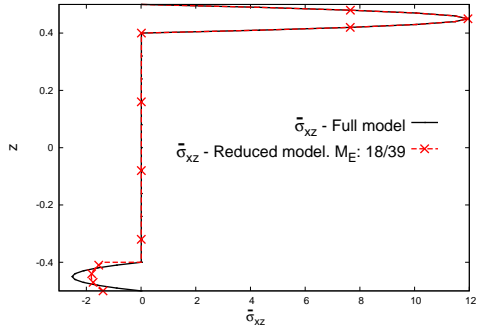


(a) Stress  $\bar{\sigma}_{yz}$ . Ply sequence:  $0^\circ/90^\circ/0^\circ$ .

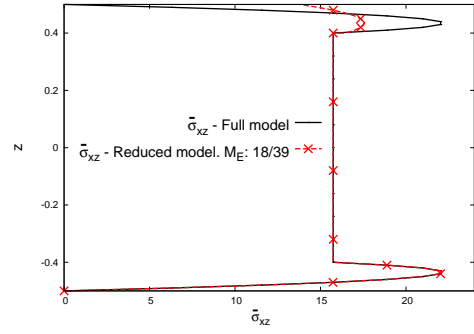


(b) Stress  $\bar{\sigma}_{yz}$ . Ply sequence:  $0^\circ/0^\circ/90^\circ$ .

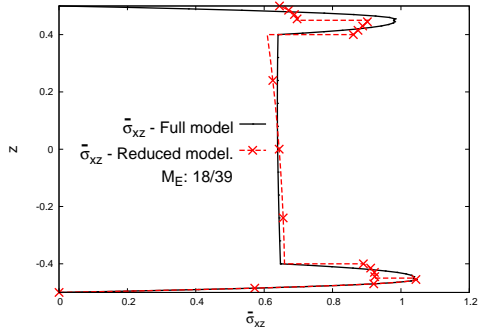
Figure 6:  $\bar{\sigma}_{xz}$  and  $\bar{\sigma}_{yz}$  vs  $z$ . Composite plate,  $a/h = 100$ . Maximum point criterium.



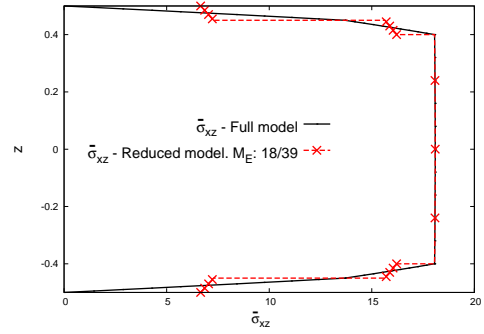
(a) Sandwich plate benchmark 2.  $a/h = 4$ .



(b) Sandwich plate benchmark 2.  $a/h = 100$ .



(c) Sandwich plate benchmark 3.  $a/h = 4$ .



(d) Sandwich plate benchmark 3.  $a/h = 100$ .

Figure 7: Sandwich benchmarks 2 and 3, reduced combined models. Maximum point criterium.